Chapter 8

Artificial Slip Surface: Potential Application in Lubricated MEMS

M. Tauviqirrahman, R. Ismail, J. Jamari and
D.J. Schipper

Additional information is available at the end of the chapter

http://dx.doi.org/10.5772/55745

1. Introduction

1.1. Background

For the last years, there has been a tremendous effort towards the development of Micro-Electro-Mechanical System (MEMS) for a wide variety of applications in aerospace, automotive, biomedical, computer, agricultural industries, electronic instrumentation, industrial process control, biotechnology, office equipment, and telecommunications. MEMS devices integrate chemical, physical, and even biological processes in micro-scale technology packages.

Stiction (a subtraction of 'static friction') in micro-system technology has been a problem ever since the advent of surface micromachining in the eighties of the last century. As the overall size of the machine is reduced, the capillary and surface tension force of liquid become large, which induce stiction rendering the devices to fail or malfunction. In particular, stiction forces created between moving parts that come into contact with one another, either intentionally or accidentally, during operation are a common problem with micro-mechanical devices. Stiction-type failures occur when the interfacial attraction forces exceed restoring forces. Consequently, the surfaces of these parts either temporarily or permanently adhere to each other, causing device malfunction or failure.

Several approaches to address the stiction between two opposing surfaces have been presented in the various literatures [1-4]. The basic approaches to prevent stiction include increasing surface roughness (topography) and/or lowering solid surface energy by coating with low surface energy materials. This includes self-assembled molecular (SAM) coatings, hermetic packaging and the use of reactive materials in the package [5].

Other attractive technique to tackle the stiction problem is by inserting a lubricant into the region around the interacting devices to reduce the chance of stiction-type failures. As is well-known, many MEMS devices include moving (sliding/rolling) surfaces and thus it is necessary to apply a lubricant between the contacting surfaces to reduce friction and wear. However, a significant barrier to the development of MEMS lubrication is the problem of achieving effective tribological performance of their moving parts. This is because the lubricant behavior is different at micro-scale compared to macro-scale. At the macroscopic level, it is well accepted that the boundary condition for a viscous fluid at a solid wall is no-slip, i.e. the fluid velocity matches the velocity of the solid boundary. While the no-slip boundary condition has been proven experimentally to be accurate for a number of macroscopic flows, it remains an assumption that is not based on physicals principles. At micro-scale level, certain phenomena must be taken into account when analyzing liquid flows such as a slip condition at solid wall boundaries.

As a consequence of the MEMS technology revolutionary application to many areas, it is possible for scientists to observe the boundary slip on micro/nano-meter scale. A variety of techniques are now available that are capable of probing lubricant flow on micro-scales and are therefore suitable for the investigation of boundary conditions. There are three techniques so far for detecting the boundary slip: nano-particle image velocimetry (NPIV) [6], atomic force microscope (AFM) [7-9] and surface force apparatus (SFA) [10]. The NPIV technique is a direct observation method with a measurement precision depending on the size of the nano-particles but with poor moderate accuracy. The AFM and SFA are indirect observation techniques based on the assumption that boundary slip takes place precisely on the interface of liquid and solid. These methods need a high accuracy boundary slip model to infer the slip velocity. Boundary slip has been observed not only for a hydrophobic surface [6, 7, 10] but also for a hydrophilic surface [8, 9]. Therefore, the slip evidence has been generally accepted and for certain cases the no-slip boundary condition is not valid.

There is a large body of literature dealing with the analysis of lubricant slip flow based on the analytical and numerical solution of molecular dynamic simulations [11, 12], Lattice-Boltzman [13, 14], and the Reynolds equation [15-23]. The accurate description of slip at the wall is very difficult and still remains a subject of intensive research. The so-called Navier slip model and the critical shear stress model are usually used to describe a boundary slip. In fact, nearly two hundred years ago Navier [24] proposed a general boundary condition that incorporates the possibility of fluid slip at a solid boundary. Navier's proposed boundary condition assumes that the velocity, u, at a solid surface is proportional to the shear stress at the surface. It reads: $u = b\,(\mathrm{d}u/\mathrm{d}z)$ where b is the slip length and $\mathrm{d}u/\mathrm{d}z$ is the shear rate. The slip length b, which is defined as the distance beyond the solid/liquid interface at which the liquid velocity extrapolates to the velocity of the solid, is used to quantify a boundary slip. If $b = 0$ then the generally assumed no-slip boundary condition is obtained. If b = finite, fluid slip occurs at the wall, but its effect depends upon the length scale of the flow. The Navier-slip boundary condition is the most widely used boundary condition with the methods based on the solution of continuum equations.

In micro-scales such as MEMS, the boundary condition will play a very important role in determining the lubricant flow behavior. Control of the boundary condition will allow a degree

of control over the hydrodynamic pressure in confined systems and be important in lubricated-MEMS. To prevent a stiction, in a controlled way, one is able to enhance, a hydrophobic/hydrophilic behavior of surfaces. If one surface is hydrophobic (slip) and the other is hydrophilic (no-slip) the sliding velocity or displacement between the surfaces is accommodated by shear at the hydrophobic surface (the lubricant is kept in the contact by the hydrophilic surface). In this way wear of the surfaces is prevented and the surfaces are able to move because stiction is prevented.

The slip situation, however, can be controlled to obtain a positive effect by surface technology. Coating and texturing technologies can be used to engineer large slip. In practice, a large slip can be made using super-hydrophobic surfaces. Such surfaces can be manufactured by grafting or by deposition of hydrophobic compounds on the initial surface at a certain zone. Super-hydrophobic surfaces were originally inspired by the unique water-repellent properties of the lotus leaf. It is the combination of a very large contact angle and a low contact-angle hysteresis that defines a surface as super-hydrophobic. Implementing the slip property (hydrophobicity) on a surface in a wide range of application for the mechanical components is of great challenge by numerous authors recently. In published works [15-23], both experimentally and numerically, slip surface is able to reduce friction force at the contacting surfaces and finally reduce energy consumption, increase component's life-time and reduce economic and environmental costs.

1.2. Problem statement

In classical liquid lubrication it is assumed that surfaces are fully wetted and no-slip occurs between the fluid and the solid boundary. In MEMS, this wetting is actually an unwanted process because it can encourage the occurrence of stiction and as a result micro-parts can not be moved [25]. It is expected that slip can reduce the friction and improve the load support. However, with respect to the engineered slip pattern, the choice of slip zone on a certain surface must be taken carefully in relation to such tribological performances. In other words, an inappropriate slip zone pattern on a certain surface or the election of inappropriate surface containing a slip situation may lead to the deterioration of the lubrication performance. How to control the boundary slip in the application of a lubricated-MEMS is one of the challenging tasks in the future. This chapter will explore the provision of a new lubrication model based on the continuum approach for moving parts in MEMS in order to improve the tribological performance of lubricated contacts. In MEMS, by lubrication, low friction force and high load support are the goals which want to be achieved. The artificial slip surface will be introduced as one of the solutions to improve the lubrication performance of MEMS so as MEMS with a longer life-time can be obtained. The term "artificial slip surface" is used to address a non-homogeneous engineered slip/no-slip pattern, i.e. a surface consisting of a slip zone and a no-slip zone.

2. Research methods

Full film lubrication of lubricated contact is often described by the Reynolds theory [26]. According to the classical Reynolds theory, no-slip boundary is assumed and the convergent

geometrical wedge is one of the most important conditions to generate hydrodynamic pressure. Therefore, the lubrication model for lubricated MEMS will be an extension of the classical lubrication theory. This means that modeling the lubricant through very narrow gap, normally modeled by assuming no-slip at the boundaries will be modified by introducing a boundary slip.

2.1. Modified reynolds equation

The classical Reynolds equation that is valid under no-slip condition can be generalized for taking into account slip conditions. It is then possible, for any film height distributions, to calculate the pressure distribution and the shear rate profile. The model of lubrication presented here is based on the fact that slip of the lubricant will exist at the interface of a lubricated sliding contact. Thus, a boundary slip is employed both on the moving and stationary surface, see Figure 1. The proposed lubrication model with slip leads to a modified Reynolds equation as presented in Eq. (1).

$$\begin{aligned}&\frac{\partial}{\partial x}\left(\frac{h^3}{12\mu}\frac{h^2+4h\mu\left(\alpha_t+\alpha_b\right)+12\mu^2\alpha_t\alpha_b}{h\left(h+\mu\left(\alpha_t+\alpha_b\right)\right)}\frac{\partial p}{\partial x}\right)=\frac{u_w}{2}\frac{\partial}{\partial x}\left(\frac{h^2+2h\mu\alpha_t}{h+\mu\left(\alpha_t+\alpha_b\right)}\right)\\&-u_w\frac{\alpha_t\mu}{h+\mu\left(\alpha_t+\alpha_b\right)}\frac{\partial h}{\partial x}+\frac{h}{2\mu}\frac{\partial p}{\partial x}\frac{\partial h}{\partial x}\frac{h\alpha_t\mu+2\alpha_t\alpha_b\mu^2}{h+\mu\left(\alpha_t+\alpha_b\right)}\end{aligned} \tag{1}$$

The physical meanings of the symbols in Eq. (1) are as follows: h the lubrication film thickness (gap) at location, p the lubrication film pressure, μ the lubricant viscosity, α the slip coefficient (subscripts t and b denote the top (stationary) and bottom (moving) surface, respectively) and u_w the velocity of the moving surface. It can be seen in that if the slip coefficient α is set to zero (no-slip condition), Eq. (1) reduces to the classical Reynolds equation. It should be noted that the product of multiplication of the slip coefficient by the viscosity, $\alpha\mu$, is usually called as 'slip length' b.

Eq. (1) is derived by following the usual approach to deduce the Reynolds equation from the Navier-Stokes system by assuming classical assumptions except that boundary slip is applied both on the stationary surface and moving surface as depicted in Figure 1.

Eq. (1) can be derived by considering the equilibrium of an element of fluid.

$$\frac{\partial^2 u}{\partial z^2}=\frac{1}{\mu}\frac{\partial p}{\partial x} \tag{2}$$

where z lies along the direction across the thickness of the film, and u is the velocity field. To obtain the velocity profile, Eq. (2) can be integrated twice.

http://dx.doi.org/10.5772/55745

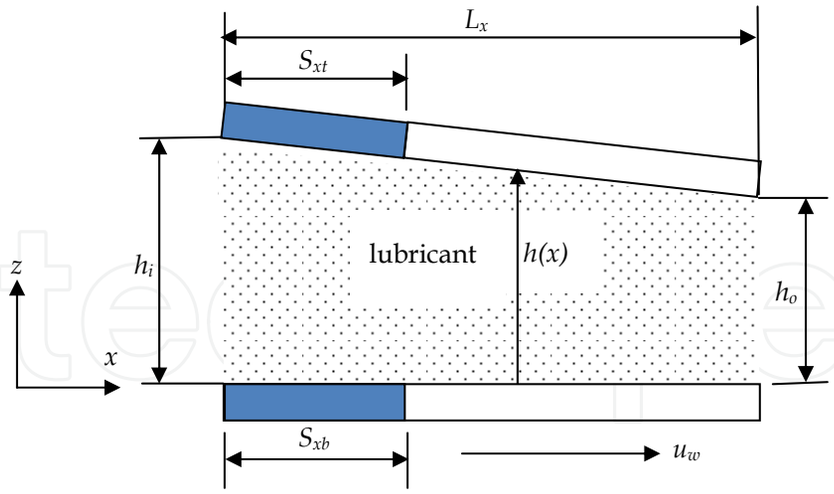

Figure 1. Schematic of a lubricated sliding contact with artificial slip surface applied both on the stationary and the moving surface. The boundary slip zones (S_{xt} and S_{xb}) are located at the leading edge of the contact. (Note: u_w is the sliding velocity, L_x is contact length, h_i and h_o are inlet and outlet film thickness, respectively, $h(x)$ is variable film thickness).

$$u = \frac{1}{2\mu}\frac{\partial p}{\partial x}z^2 + C_1 z + C_2 \tag{3}$$

C_1 and C_2 in this case are either constants or functions of x and can be solved by applying a boundary condition for u. The bottom and the top surfaces have the slip condition based on slip length model.

$$\left.\begin{aligned} &at\ z=0,\ u = u_w + \alpha_b \mu \left.\frac{\partial u}{\partial z}\right|_{z=0} \\ &at\ z=h,\quad u = -\alpha_t \mu \left.\frac{\partial u}{\partial z}\right|_{z=h} \end{aligned}\right\} \tag{4}$$

This gives

$$u = \frac{1}{2\mu}\frac{\partial p}{\partial x}z^2 - \left(\frac{u_w}{h+\mu\left(\alpha_t+\alpha_b\right)} + \frac{h}{2\mu}\frac{\partial p}{\partial x}\frac{h+2\alpha_t\mu}{h+\mu\left(\alpha_t+\alpha_b\right)}\right)z + u_w\frac{h+\alpha_t\mu}{h+\mu\left(\alpha_t+\alpha_b\right)} \tag{5}$$

$$-\frac{h}{2\mu}\frac{\partial p}{\partial x}\frac{\alpha_b\mu(h+2\alpha_t\mu)}{h+\mu\left(\alpha_t+\alpha_b\right)} \tag{6}$$

This velocity is used to compute the flow rate, q by integrating across the fluid film thickness, h. When q is differentiated to fulfill the continuity of flow, assuming μ is constant; this gives a modified Reynolds equation as stated in Eq. (1).

When full film lubrication is assumed, the entire load w is carried by the lubricant film and the calculation is simply an integration of the lubricant film pressure distribution over contact area, i.e.

$$w = \int_0^{L_x} p(x)dx \tag{7}$$

The friction force f generated by the lubrication system is due to the fluid viscous shear. It is calculated by integrating the shear stress over the surface area. These shear stresses are given by

$$\tau(x,z) = \left(\mu \frac{\partial u}{\partial z}\right)_{z=h} \tag{8}$$

The simulation results will be presented in dimensionless form, i.e. $P = ph_o^2 / \mu L_x u_w$ for the dimensionless pressure, $W = wh_o^2 / (u_w \mu L_x^2)$ for the dimensionless load support (where w is the load per unit width), $F = f h_o / \mu u_w L_x$ for dimensionless friction force (where f is the friction force per unit width), and $m = F / W$ for dimensionless friction coefficient. In the present study, the dimensionless slip length A is determined by normalizing the slip length b with the outlet film thickess h_o. For slip analysis in the following computations, the dimensionless slip length A varies from 3 to 300, which are reasonable values of the slip length based on the results published in literature [17, 18, 20].

2.2. Solution method

The modified Reynolds equation, Eq. (1) is discretized over the flow using the finite volume method, and is solved using the tridiagonal matrix algorithm (TDMA), [27]. By employing the discretization scheme, the computed domain is divided into a number of control volumes using a grid with uniform mesh size. The grid independency is validated by various numbers of mesh sizes. An assumption is made that the boundary pressures are zero at both sides of the contact.

A numerical simulation is conducted to investigate the possible application so as a boundary slip can be beneficial to achieve a high load support and low friction force. In order to maximize the performance of lubrication, the boundary conditions (slip zones, S_{xt} and S_{xb}, see Figure 1) of the model are optimized through a parametric analysis. The object of optimization is to maximize the hydrodynamic load support. The load support satisfies two main functional purposes: (a) carry the applied external load, and (b) to minimize the contact between the opposing solids, and thus wear. The optimization analysis attempts to satisfy both functional requirements with a single design parameter, the slip zone.

http://dx.doi.org/10.5772/55745

The parametric analysis is performed using a developed computer code to investigate the effect of various slip parameters on the lubrication performances (load support, friction force, and friction coefficient). A parametric study is conducted with the variation of slip parameters (slip zone and slip length) over a large range of values considering different performance parameters. The design variables and the objective function are referred to as the optimization variables. The design variables are independent quantities which are varied in order to achieve the optimum design. The objective function is the dependent variable that is maximized, i.e. the load support. In the present study, the design variables are slip zones as indicated in Figure 1. The algorithm used in the present study is depicted on Figure 2.

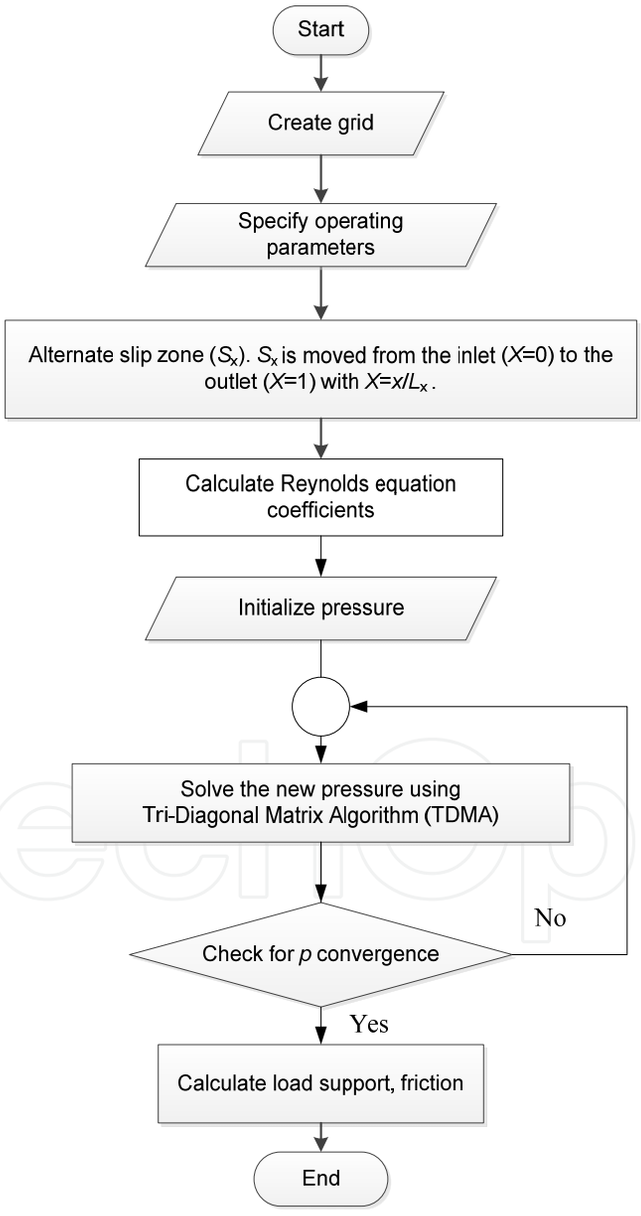

Figure 2. Flow chart for numerical method.

3. Key results

The behavior of traditional (no-slip) hydrodynamic lubrication between the opposing surfaces can be estimated by a classical form of the Reynolds equation. The derivation of the classical Reynolds equation is based on the assumption of no-slip between the lubricant and the surfaces. In the classical Reynolds lubrication, the mechanism to generate a pressure is due to the convergent wedge effect. An artificial slip surface presented here is designed to be able to carry the external load during lubrication even if the wedge effect is not present. This situation is very beneficial in designing lubricated-MEMS which exhibits parallel gaps.

In this chapter, there are two main investigations. At first, the study is conducted in order to validate the developed numerical scheme. It assures that the numerical method used can be employed for solving other hydrodynamic characteristics. The no-slip case of lubricated contact is of main interest due to the availability of the analytical solution. Secondly, the study will be extended to explore the effect of the slip zone of the artificial slip surface on pressure, load support, friction force, and friction coefficient. The comparison between the modified sliding contact containing an artificial slip surface and the traditional one is conducted in order to describe the benefit of the use of an artificial slip pattern quantitatively.

3.1. No-slip condition

The modified Reynolds equation (Eq. (1)) is the governing equation for the fluid lubrication system containing a boundary slip. If the slip coefficient, α, is set to zero, Eq. (1) reduces to the classical Reynolds equation. In this section, in order to validate the developed computer code containing a numerical scheme using finite volume method combined with tridiagonal matrix algorithm (TDMA), the classical Reynolds equation (no-slip condition) is solved numerically for calculating the pressure distribution, and finally the friction in a lubricated sliding contact as depicted in Figure 1 and Table 1, respectively. These results are compared with the analytical solution based on the work of Cameron [28] as follows:

$$p = \frac{6u_w \mu L_x}{h_o^2} \frac{K\frac{x}{L_x}\left(1-\frac{x}{L_x}\right)}{(2+K)\left(1+K-K\frac{x}{L_x}\right)^2} \tag{9}$$

for the pressure distribution where $K = (h_i / h_o) - 1$, and

$$f = \frac{L_x \mu u_w}{h_o}\left(\frac{4\ln(1+K)}{K} - \frac{6}{(2+K)}\right) \tag{10}$$

for the friction force per unit width.

http://dx.doi.org/10.5772/55745

In Figure 3 the numerical results obtained with TDMA as well as analytical results for the dimensionless pressure distribution along the bottom wall of the contact are shown alongside those obtained from the Reynolds approximation. The wedge ratio h^* of 2.2 was considered based on the fact that a maximum load support for a no-slip contact occurs when $h^* = 2.2$ [28]. In the present study the wedge ratio h^* is defined as the inlet film thickness over the outlet film thickness, h_i/h_0, and sometimes quoted as slope incline ratio in other literature. It is observed from Figure 3 that the maximum error is within 0.01% between the pressure obtained from the analytical solution and the numerical result.

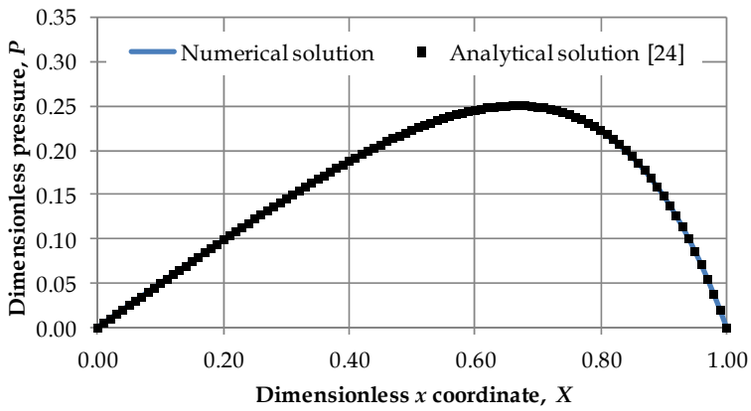

Figure 3. Normalized pressure distribution along the bottom wall of the linear wedge with no-slip boundary condition for an optimal wedge ratio h^* of 2.2.

The comparison between the dimensionless friction force F obtained with the numerical prediction and the analytical solution are presented in Table 1. Like the result of the pressure distribution, the predicted dimensionless friction force shows very good agreement with the analytical solution. In general, the numerical solution of the classical Reynolds equation is matched well with the analytical solution. It assures that the numerical method used is valid and thus can be extended for analysing other hydrodynamic characteristics.

	Dimensionless friction force, F
Analytical solution [28]	0.77
Numerical prediction [present study]	0.77

Table 1. The comparison between the analytical solution performed by Cameron [28] and the numerical simulation code.

3.2. Artificial slip surface

In MEMS, liquid lubrication has generally been omitted due to high hydrodynamic friction force that occurs in fluid film. Compared with a solid coating, stiction prevention using liquid lubrication is less practical. However, recent studies have demonstrated that it is possible for

Newtonian liquids to slip along very smooth solid walls [20] and this result may make liquid lubricants for MEMS devices feasible. The main advantage of a liquid lubricant over a solid lubricant is that they generally produce no-contact shear stresses. Unfortunately, a stiction-type failure due to a large shear and capillary forces occurs. In [15, 16], a lubrication model of low load contacts was proposed to reduce such stiction or friction. The idea behind that work was how to use a lubricant that does not wet one of the solid surfaces. It was found that a half-wetted bearing generates a significant friction reduction compared to a traditional bearing.

In order to reduce stiction, two principal methods are available, chemical and physical modification of the surfaces. To generate wall slip, in the chemical approach, the chemical composition of the surface is altered. In the physical approach, the surfaces are roughened to decrease the effective contact area [29].

In practice, the slip zone of the artificial slip surface can be prepared from (super)hydrophobic surface which uses chemical properties as well as micro- and nano-structures in order to achieve a high level of friction force reduction. The main characteristic of (super)hydrophobic surfaces is the slip length. Extensive studies have confirmed that the chemical treatment of the surfaces generates a slip length in the order of 1 μm [30], while longer slip length up to 100 μm can be obtained through a combination of a hydrophobic surface with textured structure [20, 31, 32]. In the present study, it will be shown by the computational analysis that a longer slip length applied on the slip zone of the artificial slip surface leads to a greater friction force reduction in combination with an improved load support.

3.2.1. Beneficial surface of slip

Recently, the use of an engineered slip surface has become popular with respect to lubrication, since this type of surface enhancement would give a better tribological performance. The great challenge for an engineered slip surface from the perspective of a numerical simulation is choosing the optimal slip zone geometry with respect to the lubrication performance. Two engineered slip surface modes were used currently: homogeneous slip surface (i.e. slip applied over the whole surface) and artificial slip surface (i.e. surface consisting of slip zone and no-slip zone). It can be noted that term "artificial slip surface" was sometimes also called as heterogeneous slip/no-slip surface [17, 18] and mixed slip surface [19]. The first study to mention using a homogeneous slip was dedicated by Spikes [15, 16] who numerically studied the effect of slip profiles on friction. The author pointed out that by introducing the half-wetted bearing having a homogeneous slip boundary on one of the surfaces, a reduced friction can be obtained. Subsequently, an experimental study was published in [20] confirming the finding of [15, 16]. However, in addition to the friction reduction, it was shown that a homogeneous slip surface usually has a negative effect, i.e. the decrease in the load support. If the lubricated contact exhibits a perfect slip property, it was found that the fluid load support was only half of that without slip [115, 19, 21, 23]. Clearly, this is unwanted effect with respect to the lubrication. Therefore, to date, an artificial slip surface has become of great interest by some researchers [17-19, 21, 23] with the focus of how to balance the slip effect on the load support and friction.

The big question with respect to the tribological performance of lubricated-MEMS emerges in accordance with at which wall boundary slip must be applied, at the stationary surface, moving

http://dx.doi.org/10.5772/55745

surface, or both of them. Besides that, the types of slip zone pattern become also great issue. Therefore, a series of simulations were conducted with such boundaries to find the best possibility of slip boundary application in terms of load support. Investigations were made for four kinds of slip boundaries to find the best boundary slip in terms of tribological performance, i.e. (1) slip applied on both the stationary and moving surfaces is referred as 'condition 1', (2) slip applied on the stationary surface is referred as 'condition 2', (3) slip applied on the moving surface is referred as 'condition 3', and (4) no-slip condition applied on the both of surfaces is referred as 'condition 4'. Here, a homogeneous slip surface is employed for all slip conditions.

Figure 4 presents the effect of the wedge ratio h^* on the dimensionless load support W. It is shown that the contact with homogeneous slip condition of 1, 2, and 3 have a negative effect, i.e. a reduced load support. The highest achievement of a load support W is obtained when the slip is applied on the stationary surface (condition 2). However, the value of the predicted load support is much lower than the conventional lubricated contact for all values of wedge ratio. It is only half of what the conventional Reynolds theory predicts for an optimal wedge ratio of a traditional slider contact. Fortunately, the direct trend of homogeneous slip to decrease the load support W is counterbalanced by the fact that such surface also reduces friction significantly. This is indicated in Figure 5 which shows the comparison between the dimensionless friction F for condition 2 and the condition 4 for the range of wedge ratio, h^*. The reduced friction as an advantageous effect in the lubrication can be explained by the fact that the boundary slip tends to reduce the wall shear rate at a prescribed film thickness, and then the wall shear stress and friction. Therefore, in the following design for the maximal lubrication performance, the lubricant has a no-slip boundary condition at the moving solid surface but can slip along the stationary surface. In the next section, the geometry of the boundary slip zone making an artificial slip surface will be investigated in order to achieve a higher load support as well as a low friction force.

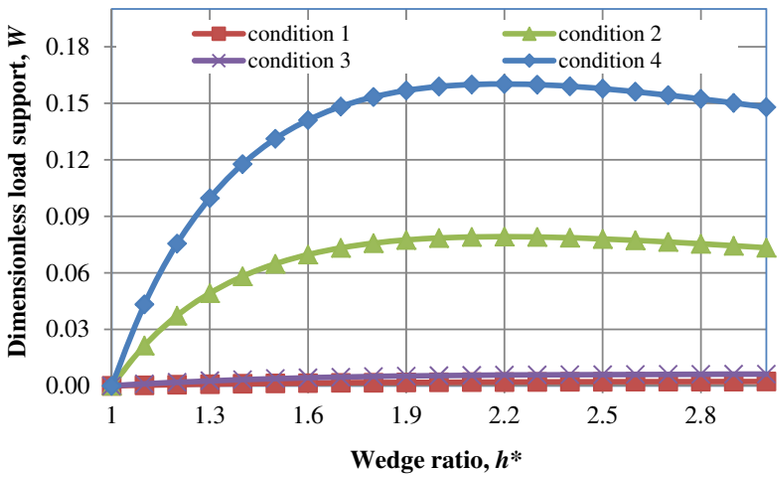

Figure 4. Dimensionless load support versus wedge ratio for several homogeneous boundary slip conditions. (Note: slip on stationary and moving surfaces (condition 1); slip on stationary surface (condition 2); slip on moving surface (condition 3); traditional no-slip (condition 4)). For the slip cases, the dimensionless slip length A of 20 is assumed.

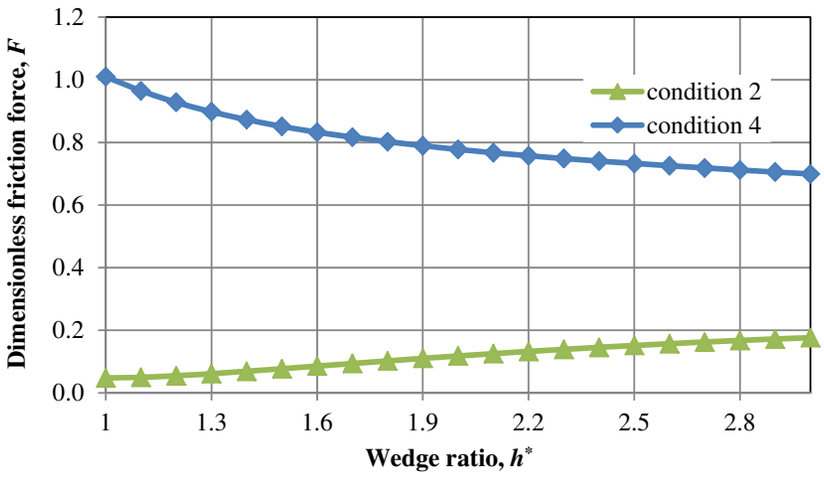

Figure 5. Dimensionless friction force versus wedge ratio at boundary condition in which slip applied on the stationary surface (condition 2) compared to the no-slip condition (condition 4).

3.2.2. The optimum slip zone of the artificial slip surface

This section is intended to investigate the optimum slip zone of the artificial slip surface for several values of wedge ratios h^* with respect to the load support.

In the following computations, as discussed in the previous section, for a high load support, it is considered that the artificial slip surface will take place on the stationary surface, whereas no-slip condition occurs on the moving surface. The parameter S_{xD} (in which $S_{xD} = S_x/L_x$) is introduced in order to completely define the dimensionless slip zone. A parametric analysis is conducted by varying the dimensionless slip zone S_{xD} from zero (i.e. no-slip boundary) to one (i.e. homogeneous boundary slip). The effect of slip zone geometry on the load support is presented in Figure 6. It can be shown that the load support has a maximum value when S_{xD} = 0.65 and h^* = 1 (i.e. parallel sliding surfaces). It should be noted that no hydrodynamic pressure can be built up in parallel sliding surfaces for traditional no-slip contact. From Figure 6, it is also shown that with the increase in wedge ratio h^*, a clear shift of the maximum load support toward to outlet can be observed in this work. In addition, the maximum load support decreases with the increase in h^*. A first conclusion is that for the best artificial slip surface with respect to the load support performance, the slip zone must be employed on the leading edge of the parallel sliding contact.

Figure 7 shows the normalized representation of lubrication film pressure distributions as a function of wedge ratio which are predicted by the modified Reynolds equation (Eq. (1)). For slip configuration, the optimal slip zone S_{xD} of 0.65, is employed. It can be shown that compared with the no-slip boundary condition, the artificial slip surface yields a positive fluid pressure. However, the performance improvement obtained through artificial slip surface is rather mild for the high wedge ratio. Obviously, the lower the base geometry wedge ratio (thus leads to the parallel sliding contact), the larger improvement that boundary slip can induce. In other words, using the artificial slip surface considered here, the maximum pressure occurs not at a

http://dx.doi.org/10.5772/55745

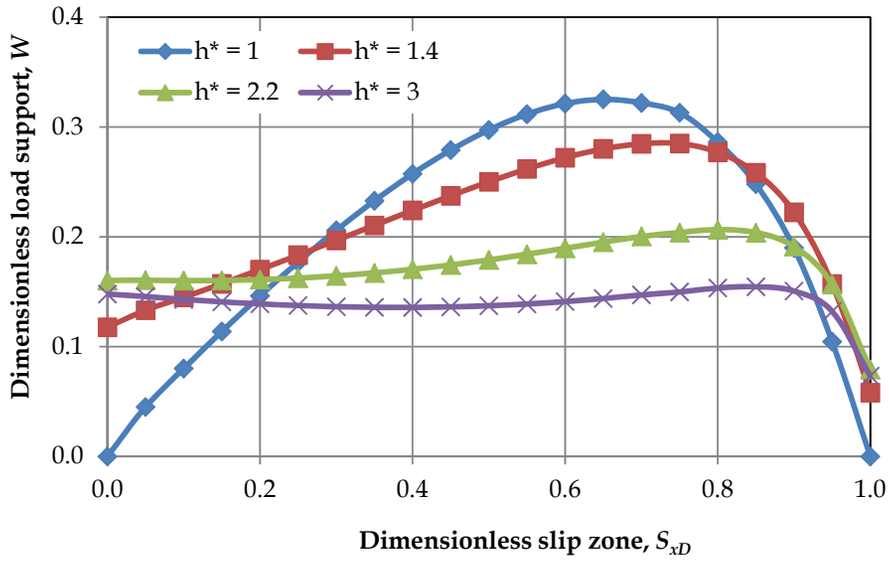

Figure 6. Effect of the dimensionless slip zone of the artificial slip surface S_{xD} on the dimensionless load support W for several wedge ratios h^*.

convergent wedge as predicted by the classical Reynolds assumption ($h^*_{opt} = 2.2$ [28]), but at a parallel surface. The predicted maximum pressure for a parallel gap is over three times as large as the maximum pressure obtained from a no-slip contact when the wedge ratio $h^* = 2.2$. From this perspective, the well-chosen artificial slip surface pattern can be considered as a potential application which is possible for lubricated-MEMS based devices with respect to the load support. In this way, liquid lubricants on the modified opposing surfaces (i.e. artificial slip surface) can prevent the lubrication to break down during device operation to the point where they no longer give proper lubrication.

Figure 8 shows the dimensionless surface friction force F at the bottom surface. It can be seen that the friction of the artificial slip surface becomes smaller than that of a traditional no-slip lubricated contact especially when S_{xD} is larger than about 0.6. This agrees with the numerical analysis of Wu *et al*. [19] eventhough the slip model and numerical method used are different. One can remark that when there is no wedge effect (i.e. $h^* = 1$) and $S_{xD} = 0.65$, the artificial slip surface gives the minimum dimensionless friction force of 0.65, while the no-slip lubricated contact gives its dimensionless minimum friction of 0.77 at $h^*_{optimal} = 2.2$, see Table 1. It means that the optimized artificial slip surface of lubricated-MEMS can produce a lower friction force than a no-slip contact.

3.2.3. Effect of dimensionless slip length on lubrication performance

The hydrophobicity of a solid surface, as discussed in the previous section, is usually expressed in terms of a slip length, which quantifies the extent to which the fluid elements near the surface are affected by the surface energy and the surface geometry. The surface energy is an intrinsic property of a material that can be controlled by chemical treatment, such as etching approach and/or coat-on/cast approach. The surface roughness of a hydrophobic solid material can be

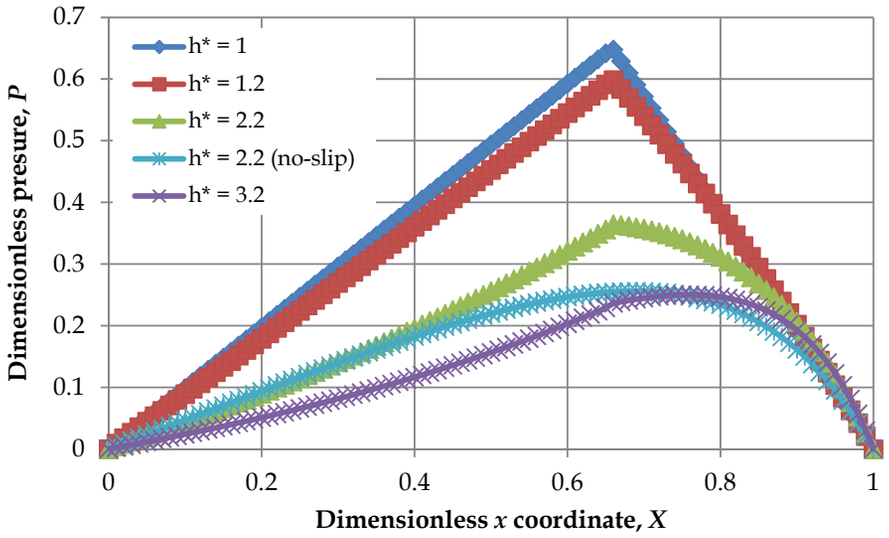

Figure 7. Lubrication film pressure distributions for several values of wedge ratio. The slip profiles are calculated for optimized dimensionless slip zone S_{xD} = 0.65 and dimensionless slip length A = 20.

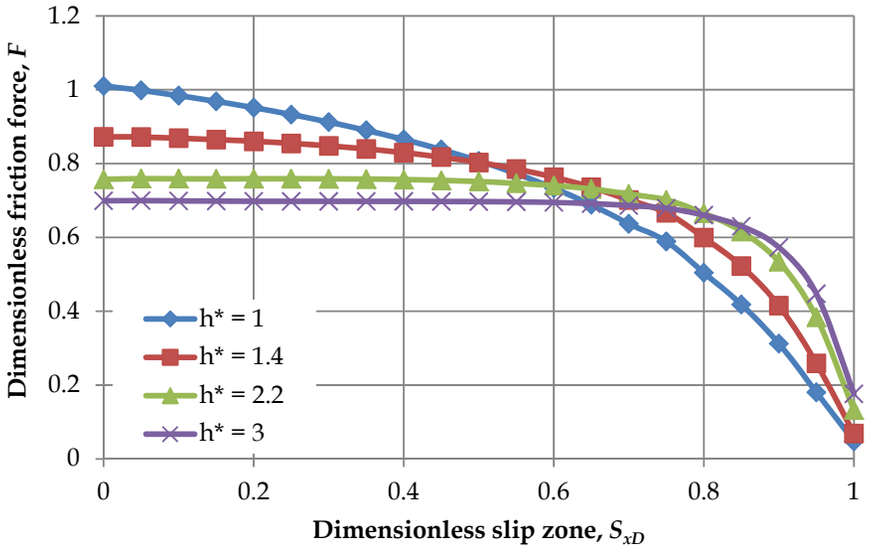

Figure 8. Effect of the dimensionless slip zone of the artificial slip surface S_{xD} on the dimensionless friction force F at bottom surface for several values of wedge ratio h^*. The slip profiles are evaluated for dimensionless slip length A = 20.

tuned in order to increment its hydrophobicity and obtain a super-hydrophobic solid surface [33, 34]. In this section, from the numerical point of view, the effect of slip length on the lubrication behavior is studied. The dimensionless slip length is varied from 3 to 300.

Figure 9 shows the effect of slip zone of the artificial slip surface for several dimensionless slip length values on the dimensionless load support. As indicated in Figure 9, the increase in the slip length leads to an increase in the predicted load support. Generally, the larger the slip length at the optimized slip zone of the artificial slip zone, the higher the load support.

http://dx.doi.org/10.5772/55745

However, when dimensionless slip length is larger than 30, the dimensionless load support is not affected significantly with the increase in the dimensionless slip length. So, the increase of the load support is not infinitely large. It can be deduced that there is no fluid load support for a lubricated-MEMS when it contains no-slip condition ($A = 0$). It indicates that the absence of the wedge effect on the pressure generation at parallel lubricated sliding contact has been counterbalanced by the influence of the aritical slip surface application. Again, this condition is very advantageous in engineering a lubricated-MEMS which demonstrates parallel gaps.

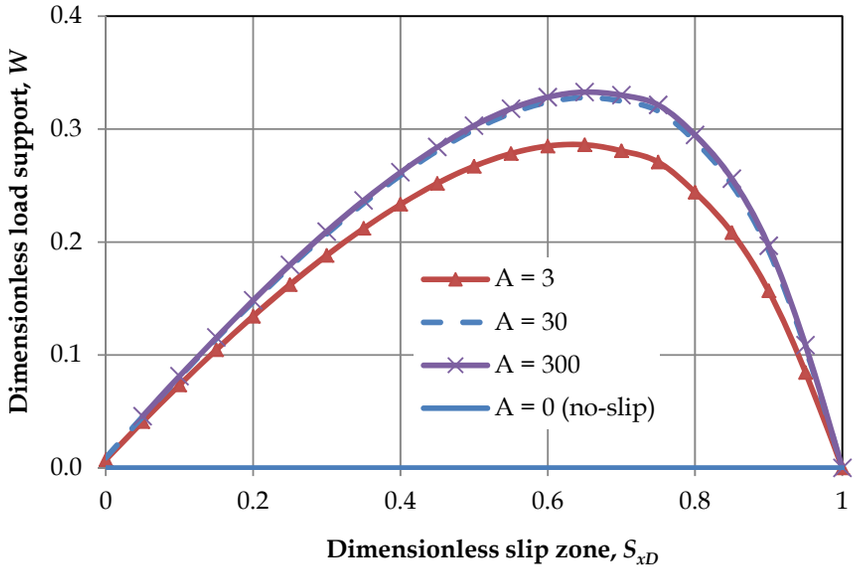

Figure 9. Effect of the dimensionless slip zone of the artificial slip surface S_{xD} on the dimensionless load support W for several values of dimensionless slip length A. All profiles are calculated for parallel sliding surfaces ($h^* = 1$).

In Figure 10 the effect of slip zone of the artificial slip surface for several dimensionless slip length values on the dimensionless friction force is presented. As is well-known, the ability to control and manipulate friction force during sliding is extremely important key to prolong a life-time of lubricated-MEMS. Better understanding of the friction force phenomena at micro-scales is needed to provide designers and engineers the required tools and capabilities to control friction force and predict failure of lubrication in MEMS.

As can be seen in Figure 10 that the artificial slip surface leads to a reduction of the friction force for all dimensionless slip length. The friction force decreases with increasing the slip zone S_x. It can be seen that when the slip zone covers over the whole surface, i.e. homogeneous slip surface, the friction forces has a minimum value, especially for a high slip length. If the reduction in friction force is of only particular interest, the homogeneous slip surface ($S_{xD} = 1$) is very beneficial. But if the performance is also related to the load support, homogeneous slip is not recommended because when $S_{xD} = 1$, the predicted load support is very small for all wedge ratios, see Fig. 6. With respect to the influence of the dimensionless slip length, opposite to the hydrodynamic load support, the dimensionless friction force becomes smaller for higher dimensionless slip length. Therefore, the optimized artificial slip surface is a very promising

way to increase the hydrodynamic performance and the stability of the lubricated MEMS system because it gives an advanced load support in combination with a reduced friction force.

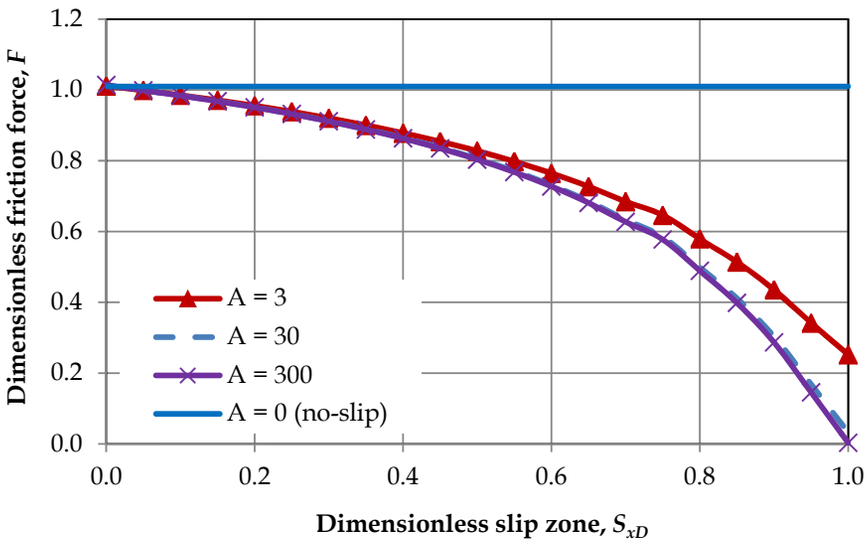

Figure 10. Effect of the dimensionless slip zone of the artificial slip surface S_{xD} on the dimensionless friction force F for several values of dimensionless slip length A. All profiles are calculated for parallel sliding surfaces ($h^* = 1$).

The combined effect of slip zone parameter on load support and friction force can be better analyzed using the dimensionless friction coefficient. In the present study the dimensionless friction coefficient m is defined as the ratio of the dimensionless friction coefficient F to the dimensionless load support W. Figure 11 shows the variation of the dimensionless friction coefficient m as a function of the dimensionless slip zone S_{xD} for various slip lengths A. It appears that when the dimensionless slip zone is smaller than 0.2, the friction coefficient increases significantly. After $S_{xD} = 0.2$, increasing the slip zone will be less significant to the reduction of the friction coefficient. It can also be deduced from Figure 11 that dimensionless friction coefficient m will decrease with the increase of the dimensionless slip length A, especially for small S_{xD}. It implies that the minimum dimensionless friction coefficient is accord with the the highest dimensionless load support (when $S_{xD} = 0.65$).

4. Concluding remarks

Numerical results show that the hydrodynamics of a lubrication film confined between a moving no-slip surface and a stationary with an artificial slip surface differ significantly from that of a film confined between two no-slip surfaces. It is found that a homogeneous slip boundary on one surface produces a lower hydrodynamic pressure in a lubricated sliding contact at various conditions (slope incline, and slip length), resulting in a reduced load support which reduces the positive effect of slip on friction. However, if the surface is designed with an optimal artificial slip pattern (the slip zone is applied on 0.65 of contact length), even

http://dx.doi.org/10.5772/55745

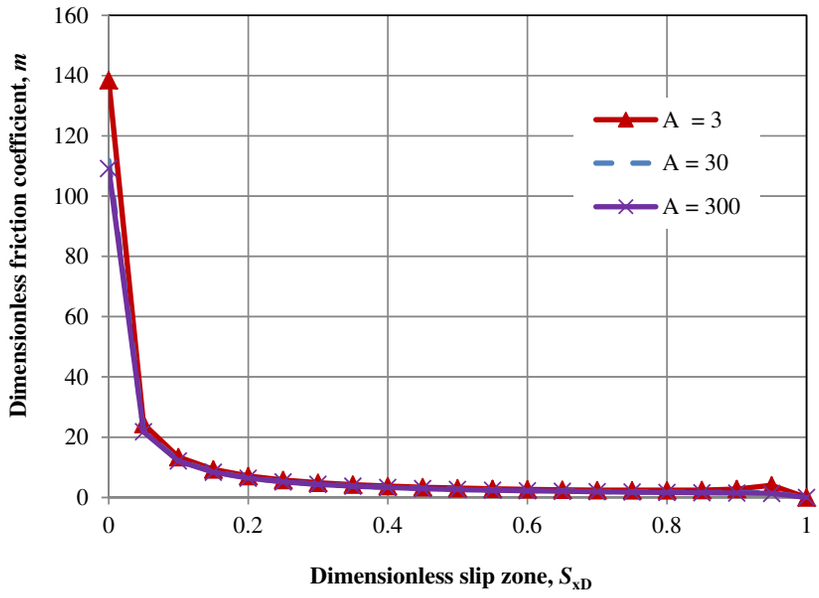

Figure 11. Effect of the dimensionless slip zone of the artificial slip surface S_{xD} on the dimensionless friction coefficient m for several values of dimensionless slip length A. All profiles are calculated for parallel sliding surfaces ($h^* = 1$).

when there is no wedge effect, the load support has a maximum value. In addition, the friction force can decrease significantly. Therefore, it is very beneficial to make one of the contacting surfaces in lubricated-MEMS with an artificial slip surface for achieving ideal lubrication performance, i.e. reduced friction coefficient and increased load support.

Author details

M. Tauviqirrahman[1,2], R. Ismail[1,2], J. Jamari[1] and D.J. Schipper[2*]

*Address all correspondence to: d.j.schipper@utwente.nl

1 Laboratory for Engineering Design and Tribology, Mechanical Engineering Department, University of Diponegoro, Jl. Prof. H. Sudharto, Kampus UNDIP Tembalang, Semarang, Indonesia

2 Laboratory for Surface Technology and Tribology, University of Twente Drienerlolaan, Enschede, The Netherlands

References

[1] Houston MR, Howe RT, Maboudian R. Effect of Hydrogen Termination on The Work of Adhesion Between Rough Polycrystalline Silicon Surfaces. Journal of Applied Physics 1997;81(8): 3474–3483.

[2] Maboudian R, Ashurst WR, Carraro C. Self-Assembled Monolayers as Anti-Stiction Coatings For MEMS: Characteristics and Recent Developments. Sensors and Actuators A: Physical 2000;82(1–3): 219–223.

[3] Tagawa M, Ikemura M, Nakayama Y, Ohmae N. Effect of Water Adsorption on Microtribological Properties of Hydrogenated Diamond-Like Carbon Films. Tribology Letters 2004;17(3): 575–580.

[4] Smallwood SA, Eapen KC, Patton ST, Zabinski JS. Performance Results of MEMS Coated with a Conformal DLC. Wear 2006;260: 1179–1189.

[5] van Spengen WM, Puers R, De wolf I. On The Physics of Stiction and Its Impact on The Reliability of Microstructures. Journal of Adhesion Science and Technology 2003;17(4): 563–582.

[6] Pit R, Hervet H, Leger L. Direct Experimental Evidence of Slip in Hexadecane: Solid Interfaces. Physical Review Letters 2000;85: 980–983.

[7] Craig VSJ, Neto C, Williams DRM. Shear-Dependent Boundary Slip in an Aqueous Newtonian Liquid. Physical Review Letters 2001;87(054504).

[8] Bonaccurso E, Kappl M, Butt HJ. Hydrodynamic Force Measurements: Boundary Slip of Hydrophilic Surfaces and Electrokinetic Effects. Physical Review Letters 2002;88(076103).

[9] Bonaccurso E, Butt HJ, Craig VSJ. Surface Roughness and Hydrodynamic Boundary Slip of A Newtonian Fluid in A Completely Wetting System. Physical Review Letters 2003;90(144501).

[10] Zhu YX, Granick S. Rate-Dependent Slip of Newtonian Liquid at Smooth Surfaces. Physical Review Letters 2001;87(096105).

[11] Priezjev NV, Darhuber AA, Troian SM. Slip Behaviour in Liquid Films on Surfaces of Patterned Wettability: Comparison Between Continuum and Molecular Dynamics Simulations. Physical Review E 2005;71(041608).

[12] Cottin-Bizonne C, Barentin C, Charlaix E, Bocquet L, Barrat JL. Dynamics of Simple Liquids at Heterogeneous Surfaces: Molecular Dynamics Simulations and Hydrodynamic Description. European Physical Journal E 2004;15: 427– 438.

[13] Harting J, Kunert C, Herrmann HJ. Lattice Boltzmann Simulations of Apparent Slip in Hydrophobic Channels. Europhysic Letters 2006; 75: 328–334.

[14] Li BM, Kwok DY. Discrete Boltzmann Equation for Microfluidics. Physical Review Letters 2003;90(124502).

[15] Spikes HA. The Half-Wetted Bearing. Part 1: Extended Reynolds Equation. Proceedings of the Institution of Mechanical Engineers, Part J: Journal of Engineering Tribology 2003; 217: 1–14.

[16] Spikes HA. The Half-Wetted Bearing. Part 2: Potential Application in Low Load Contacts. Proceedings of the Institution of Mechanical Engineers, Part J: Journal of Engineering Tribology 2003;217: 15–26.

[17] Salant RF, Fortier AE. Numerical Analysis of A Slider Bearing with A Heterogeneous Slip/No-Slip Surface. Tribology Transactions 2004; 47: 328–334.

[18] Fortier AE, Salant RF. Numerical Analysis of A Journal Bearing with A Heterogeneous Slip/No-Slip Surface. ASME Journal of Tribology 2005;127: 820–825.

[19] Wu CW, Ma GJ, Zhou P. Low Friction and High Load Support Capacity of Slider Bearing with A Mixed Slip Surface. ASME Journal of Tribology 2006;128: 904–907.

[20] Choo JH, Glovnea RP, Forrest AK, Spikes HA. A Low Friction Bearing Based on Liquid Slip at The Wall. ASME Journal of Tribology 2007;129: 611–620.

[21] Tauviqirrahman M, Ismail R, Jamari, Schipper DJ. Effect of Boundary Slip on The Load Support in A Lubricated Sliding Contact. AIP Conference Proceedings 2011;1415: 51-54. doi:10.1063/1.3667218.

[22] Aurelian F, Patrick M, Mohamed H. Wall Slip Effects in (Elasto) Hydrodynamic Journal Bearing. Tribology International 2011;44: 868–877.

[23] Tauviqirrahman M, Ismail R, Jamari, Schipper DJ. Wall Slip Effects in a Lubricated MEMS. International Journal of Energy Machinery 2011;4(1): 13–22.

[24] Navier CLMH. Mémoire Sur Les Lois Du Mouvement Des Fluides. Mémoires de l'Académie Royale des Sciences de l'Institut de France 1823:6: 389–440.

[25] Israelachvili J. Intermolecular and Surface Force, vol. 1, second ed. Academic Press, London; 1995.

[26] Reynolds O. On The Theory of Lubrication and Its Application to Mr. Beauchamp Tower's Experiments, Including An Experimental Determination of The Viscosity of Olive Oil. Philosophical Transactions of the Royal Society of London, Part I 1886;177: 157–234.

[27] Patankar SV. Numerical Heat Transfer and Fluid Flow. Taylor & Francis, Levittown 1980:30–58.

[28] Cameron A. The Principles of Lubrication. Longman Green and Co., ltd; 1966.

[29] Kompvopoulos K. Surface Engineering and Microtribology for Microelectromechanical System. Wear 1996;200: 305–327.

[30] Tretheway DC, Meinhart, CD. Apparent Fluid Slip at Hydrophobic Microchannel Walls. Physics of Fluids 2002;14: L9-12.

[31] Watanabe K, Yanuar, Udagawa H. Drag Reduction of Newtonian Fluid in a Circular Pipe with a Highly Water-Repellant Wall. Journal of Fluid Mechanics 1999;381: 225–238.

[32] Ou J, Perot B, Rothstein JP. Laminar Drag Reduction in Microchannels using Ultrahydrophobic Surfaces. Physics of Fluids 2004;16: 4635.

[33] Patankar NA. On the Modelling of Hydrophobic Contact Angles on Rough Surfaces. Langmuir 2003;19: 1249–1253.

[34] Lafuma A, Quere D. Superhydrophobic States. Nature Materials 2003;2: 457–460.